Journal of Atmospheric and Solar-Terrestrial Physics 185 (2019) 22–28

Contents lists available at ScienceDirect

Journal of Atmospheric and Solar-Terrestrial Physics

journal homepage: www.elsevier.com/locate/jastp

Multi- decadal variations and periodicities of the precipitable water vapour (PWV) and their possible association with solar activity: Arabian Peninsula

A.H. Maghrabi

National Centre for Applied Physics, King Abdulaziz City for Science and Technology, Riyadh, 11442, Saudi Arabia

ARTICLE INFO

Keywords:
Precipitable water vapour
Trend
Solar activity
Saudi Arabia
Climate change
Mann-Kendall
Radiosonde
Periodicities

ABSTRACT

In this study, radiosonde observations from seven sites in Saudi Arabia for the period 1985 to 2016 were utilized to investigate the interannual, monthly, and seasonal variations and trends of precipitable water vapour (PWV). The magnitudes of these trends have been characterized and tested using the Mann-Kendall (MK) rank statistics at different significance levels. A significant decrease in the annual mean PWV by about 7% is found for the entire period. A seasonal cycle of PWV with a maximum during summer time and a minimum during winter has been found and can be mostly attributed to the variations of air temperature. On a monthly basis, the PWV values revealed a decreasing trend with the rate of decrease ranging between 0.47 and 2.6 mm per 32 years. There was a decrease in PWV in all the seasons, but it was only significant for the spring season, when it was the highest (1.79 mm per 32 years).

Power spectra analyses using the Fourier Transform (FT) technique were carried out for the period 1985–2016 to investigate the periodicities in the PWV time series. Several long, mid, and short-term periodicities were recognized. Short-term periodicities such as one year, six months, three months, and four months were found. On the other hand, long and mid term periodicities such as 10.8–11 years, 1.7 years, and 1.3 years were detected. The obtained periodicities are similar to those reported by several investigators and found in solar, interplanetary, and cosmic ray parameters. The spectral results suggest that the obtained PWV periodicities in Arabian Peninsula are, possibly, related to the solar activities, as well as, the effect of terrestrial meteorological phenomena.

1. Introduction

Atmospheric water content plays a crucial role in several atmospheric processes and climate change. It is the most abundant and important greenhouse gas. Water vapour absorbs both solar and terrestrial radiation, which influences the radiation exchange and radiation transfer in the atmosphere (Bevis et al., 1992; Forster and Shine, 2002; Gueymard, 1994; Maghrabi and Clay, 2010). It is considered to be one of the driving forces of the weather system and the hydrological cycle. Electromagnetic radiation from terrestrial and/or extraterrestrial origin is attenuated by the water vapour molecules.

Several atmospheric phenomena require great understanding and knowledge of the distribution and variability of atmospheric water (Gutzler, 1992; Pramualsakdikul et al., 2007).

Understanding the long-term variations and trends of atmospheric water is of great importance for several applications, such as climate change (Ruckstuhl et al., 2007; Long et al., 2000). Several researches have been conducted in different places around the world to study the long-term variations of atmospheric water (Torres et al., 2010; Zhai and Eskridge, 1997; Smirnov and Moore, 2001; Kassomenos and MCGregor, 2006; Guerova et al., 2005; Kane, 1996). However, few studies (e.g., Singh et al., 2000) of this type have been carried out in other places such as the southwest part of the Asian continent (Saudi Arabia).

In this study, the long-term trend of the total atmospheric water content (PWV) in this part of the world will be investigated and established. Data from seven sites that cover different climatic conditions will be used. The periodicities of the PWV will also be explored and established. The possible relationship between these periodicities and the solar activity will be discussed.

2. Data and methodology

2.1. Experimental data

Radiosonde observations from the record of the Saudi Presidency of Meteorology and Environment (PME) for seven sites in Saudi Arabia during the period of 1985–2016 have been used for the purpose of the current study. The selected sites are Riyadh, Abha, Medina, Jeddah,

E-mail address: amaghrabi@kacst.edu.sa.

https://doi.org/10.1016/j.jastp.2019.01.011
Received 16 December 2018; Received in revised form 22 January 2019; Accepted 23 January 2019
Available online 24 January 2019
1364-6826/ © 2019 Elsevier Ltd. All rights reserved.

Hail, Dammam, and Tabouk. These sites have been chosen because they have the longest series of observations, which are relatively homogeneous, and they cover a broad range of the climatic and atmospheric conditions experienced in the region.

The temperature, pressure, dew point temperature, and altitude of each atmospheric layer from each radiosonde profile were extracted from the surface up to 300 hPa. The termination of the data at 300 hPa was due to the poor performance of the radiosonde humidity sensors in cold temperatures (Zhai and Eskridge, 1996; Wang et al., 2002; Kassomenos and MCGregor, 2006).

Several quality control procedures were applied to the available data. These include the elimination of the whole atmospheric profile if several observations of the considered variables are missing. Radiosonde profiles with observations less than 5 km were not considered. Linear interpolation procedures were carried out to replace up to five missing profiles to complete the series. These interpolations were kept at a reasonable level in order to preserve the nature of the information contained in the data.

The total atmospheric content (PWV) was calculated for each profile according to Equation (1) (Kassomenos and MCGregor, 2006):

$$PWV = \int_0^\infty \rho_v(z)dz \tag{1}$$

where ρ_v is the absolute humidity at sounding level z and was obtained from the equation of state of an ideal gas as:

$$\rho_v(z) = \frac{217 \times RH(z) \times e(z, T)}{T} \tag{2}$$

T is the observed absolute temperature, RH (z) is the relative humidity, and e (z, T) is the saturation water vapour pressure in hPa.

PWV values were calculated separately for the day and night observations, and because diurnal variations of the PWV are not considered here, the mean PWV values of day and night times are treated as the daily mean of the PWV. This hypothesis seems to be adequate for the purposes of this study, as the main goal is to identify the PWV trends.

Table (1) summarizes some of the basic statistics of the calculated PWV for each site and the mean values. The mean PWV ranges from 13 mm, observed at three sites (Tabouk, Abha, and Hail), to 27.5 mm at the Jeddah site. The Medina and Riyadh sites exhibited the same mean values of 16 mm, while Dammam had a mean of 20 mm. The PWV for 132207 radiosonde profiles from all the sites ranged between 1.5 mm and 46.29 mm with a mean value of 17.46 mm.

The mean PWV values were binned into twelve categories to investigate the monthly variations of the PWV. Similarly, data were divided into four seasonal groups to study the seasonal variations of PWV. Winter included the months of December, January, and February; autumn included March, April, and May; June, July, and August made up the summer months; and spring included September, October, and November. Annual variations were studied by taking the twelve-month PWV values.

2.2. Analysis methods

The Mann-Kendall (MK) test and Sen's slope estimator were used to identify the presence of any trends in the PWV data. These procedures are non-parametric statistical tests that are widely used for the analysis of trends in climatologic time series (Mann, 1945; Kendall, 1975). The mathematical expression of the Kendall test statistic S is:

$$S = \sum_{i=1}^{n-1} \sum_{j=i+1}^{n} sgn(x_j - x_i) \tag{3}$$

where x_j and x_j are data values at times j and i, with $j > i$, respectively, n is the data length of the time series, and

$$\text{sgn}\,(x_j - x_i) = \begin{cases} 1 & if \quad (x_j - x_i) > 0 \\ 0 & if \quad (x_j - x_i) = 0 \\ -1 & if \quad (x_j - x_i) < 0 \end{cases} \tag{4}$$

The variance of S is calculated using Eq. (5) as:

$$V(S) = \frac{1}{18}\left[n(n-1)(2n+5) - \sum_{p=1}^{q} t_p(t_p-1)(2t_p+5)\right] \tag{5}$$

Here q is the number of tied groups and t_p is the number of data values in the group p.

The values of S and V(S) are used to compute the test statistic Z as follows:

$$Z = \begin{cases} \frac{S-1}{\sqrt{V(S)}} & if \quad S > 0 \\ 0 & if \quad S = 0 \\ \frac{S+1}{\sqrt{V(S)}} & if \quad S < 0 \end{cases} \tag{6}$$

If $|Z|$ is greater than the critical value (Z_{crit}) then the null hypothesis is invalid, implying that the trend is significant. A positive value of Z indicates an upward trend, whereas a negative value indicates a downward trend in the tested time series.

Sen's slope estimator is a nonparametric method of slope estimation. According to Sen, if a linear trend exists in a time series, then the slope can be estimated as:

$$f(t) = Qt + C \tag{7}$$

where C is a constant while Q is the slope and can be calculated from:

$$Q_{ij} = \frac{x_j - x_i}{j - i} \tag{8}$$

The median of N values of Q is represented as Sen's estimator of slope, which is given as:

$$Q_{med} = Q_{\left[\frac{N+1}{2}\right]} \text{ if N is odd} \tag{9}$$

$$Q_{med} = \frac{1}{2}\left(Q_{\left[\frac{N}{2}\right]} + Q_{\left[\frac{N+2}{2}\right]}\right) \text{ if N is even} \tag{10}$$

and is computed for all N pairs of time steps (i,j). The Q_{med} sign indicates the data trend (increase or decrease with time), while its value

Table 1
Geographical coordinates, mean, standard deviation, maximum, minimum values of the PWV (in mm), and number of radiosonde profiles used for all the sites considered during the period 1985–2016.

	Abha	Riyadh	Dammam	Hail	Jeddah	Medina	Tabouk	All
Latitude	18.24° N	24.71° N	26.39° N	27.51° N	21.28° N	24.52° N	28.38° N	
Longitude	42.51° E	46.67° E	49.97° E	41.72° E	39.23° E	39.56° E	36.56° E	
Mean	13.78	16.54	20.18	13.83	27.55	16.87	13.43	17.46
Standard deviation	6.08	6.70	9.00	5.78	9.26	7.20	5.56	8.67
Maximum	38.71	41.98	52.73	43.93	51.57	49.73	45.44	46.29
Minimum	1.07	0.21	1.04	1.16	4.16	2.16	1.17	1.5
Number of profiles	19374	19421	19120	1712	20027	18155	18990	132207

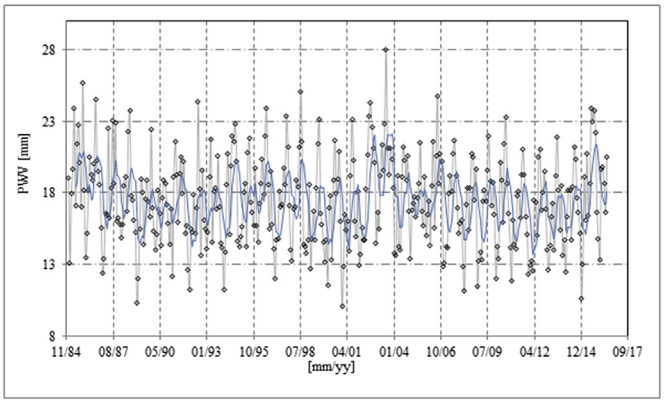

Fig. 1. Time series of monthly mean PWV during the period 1985–2016. The solid blue line is the six-month running mean.

indicates the steepness of the trend.

3. Results and discussion

3.1. General trend

Figure (1) shows the inter-annual variation of mean PWV from all stations during the considered period. Generally, the seasonal variations of the PWV are evident with spring and summer peaks and a minimum in the winter (see Fig. 4). During this period, the PWV shows its minimum value of about 10 mm in December of 1988, 2000, and 2014. On the other hand, the highest PWV (28.5 mm) was recorded in July 2003, followed by October 1985 (25.8 mm) and July 1998, when it reached a value of 25 mm.

Figure (2) indicates the trend of the annual mean values of PWV, while the results of the MK tests, Sen's slope, and total trend for all 32 years are presented in Table (2). The overall trend during the considered period is characterized by a decrease in the mean values of PWV over the study region. The estimated decrease is 0.039 mm/year (approximately 1.2 mm over the entire measurement period). This increase is statistically significant at $\alpha = 0.1$ and is about 7.15% of the overall mean PWV value (17.46 mm). During this period, the PWV varied dramatically on several occasions. The decreasing trend of the PWV from 1995 to 1992 was affected by a sharp increase of 2.5 mm from 1990 to 1991, after which it dropped again by the same value in 1992. Similarly, between 2001 and 2003, the PWV increased by about 4 mm.

During the 32-year time interval, other trends of the PWV can be

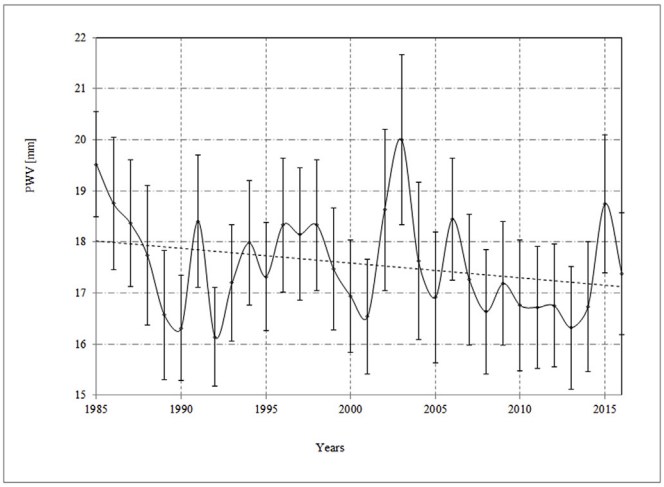

Fig. 2. Yearly mean variations of the PWV during the whole study period (1985–2016). The dashed line is the trend line.

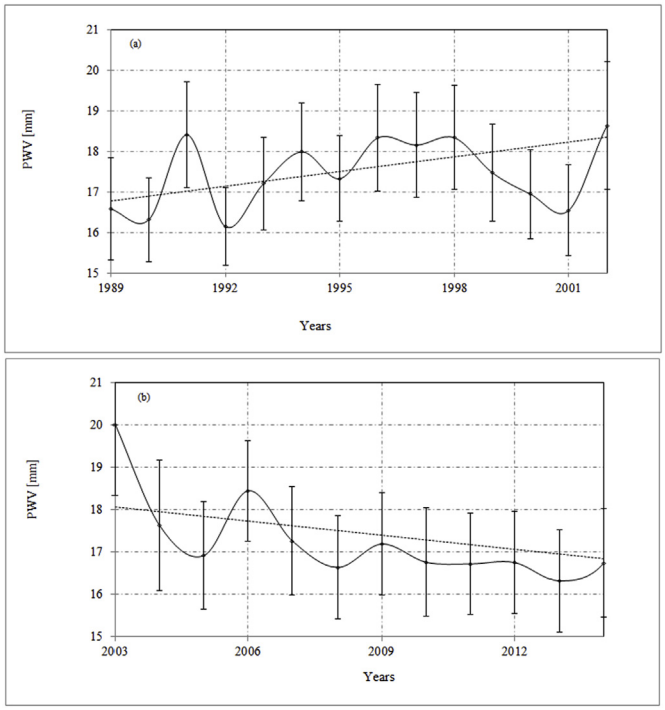

Fig. 3. Yearly variations of the PWV during the periods (a) 1989–2002 and (b) 2003–2014. The dashed line is the trend line.

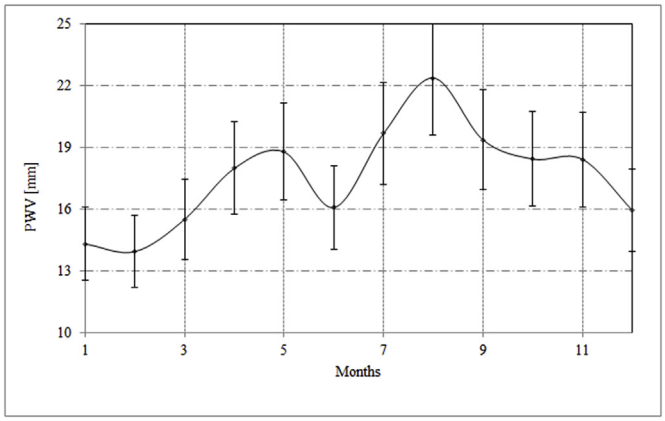

Fig. 4. Monthly variations of the PWV.

identified when the data are divided into sub-periods. The first period was from 1989 to 2002 and the second was from 2003 to 2014. Figure (3a, b) presents the trend of the PWV during these two periods and the corresponding MK results are presented in Table (2). During the first period, the PWV shows an increasing trend with a value of 0.12 mm/year. Although this period is affected by two drops during the periods of 1991–1992 and 1999–2001, the increasing trend is statistically significant at $\alpha = 0.1$ and the slope is 0.12 mm/year. Except for the dramatic increases of the PWV between 2005 and 2006, the PWV shows a significant decreasing trend with a slope of 0.19 at $\alpha = 0.01$ (99% confidence level) during the period 2003–2014.

3.2. Monthly variations

The mean monthly values of the PWV are presented in Figure (4). The general trend is similar to the trend of the air temperature (see Maghrabi and Alotaib, 2017). The PWV increases gradually from 13.9 mm in January to reach a maximum of 22.5 mm in August. Afterwards it decreases again to reach the January minimum. During

Table 2
Summary of Mann-Kendall test results, Sen Slope, and the changes in the annual PWV values for the seven sites in the selected period. Changes (%) of the PWV value compared to the 32-years mean PWV.

Period	Test Z	Significance	Sen's Slope Q	[mm/32 yrs]	Changes [%] in PWV trend compared to the average of the entire period (i.e. 17. 46)
1985–2016	−1.68	+	−0.039	−1.21	7%
1989–2002	1.69	+	0.12	+1.869	−13.194
2003–2014	−3.086	**	−0.19	−2.3222	10.621

** Trend at α = 0.01 level of significance; + trend at α = 0.1 level of significance.

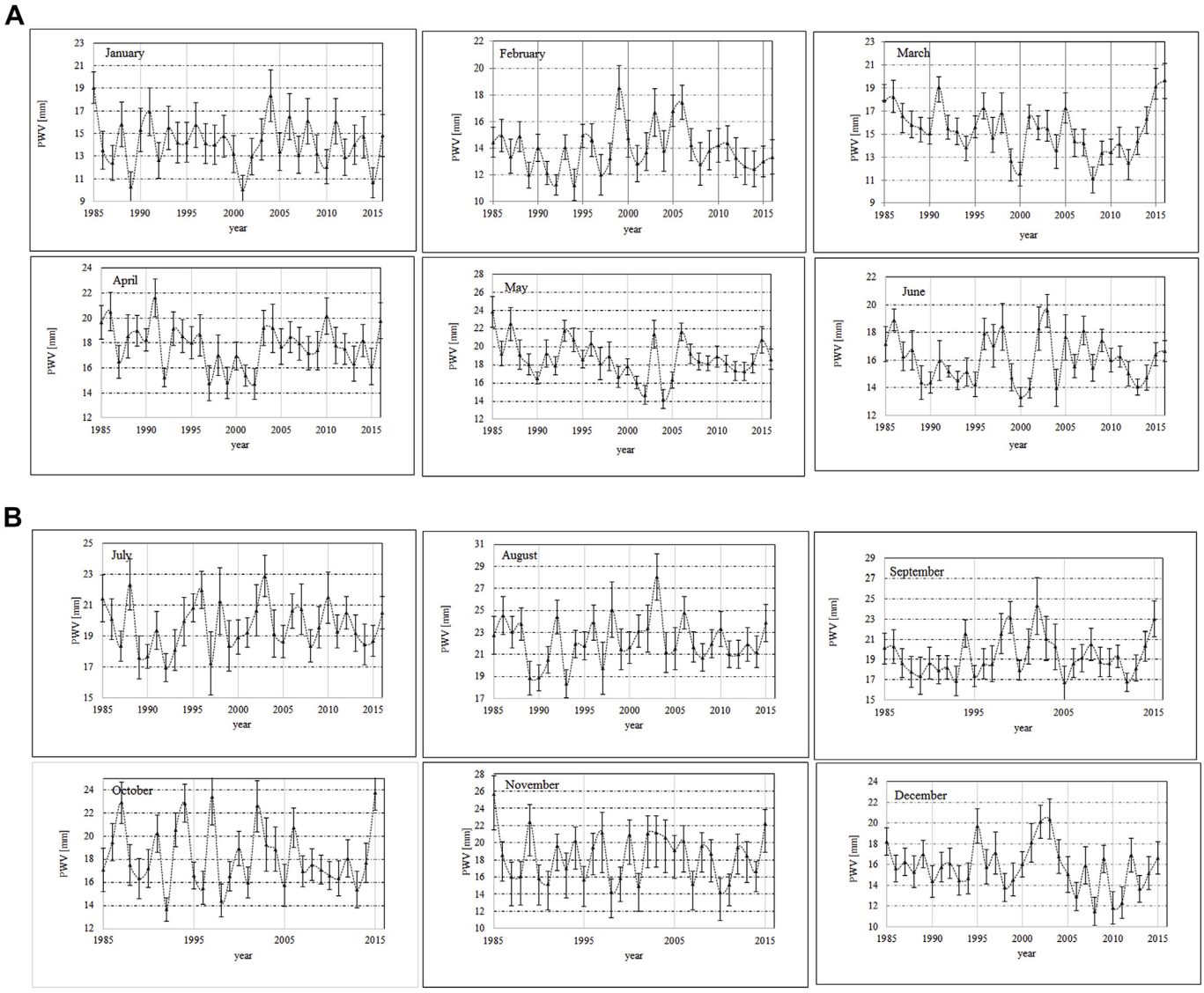

Fig. 5. Time series of the monthly mean of PWV from 1985 to 2016.

this period, a drop of by 3 mm occurs between May and June.

Figure (5) displays the variations of the PWV for each individual month during the study period. The MK tests for each month are presented in Table (3). A decreasing trend during the 32 years is observed in January, March, April, May, June, October, November, and December. On the other hand, February, July, August, and September generally presented an increasing trend in the PWV. March and May are the only two months which show significant trends at a confidence level of α = 0.1. The overall decreases in PWV in the months of March and May were, respectively, 2.6 and 1.73 mm. These values were, respectively, 16.8% and 8.8% of the mean PWV values for March and May during the 32-year period.

3.3. Seasonal variation

The mean seasonal PWV values in Saudi Arabia are characterized by high values, which mainly occur in summer, and low values in winter, generally following the temperature variation. Both transition seasons (spring and fall) showed PWV values that were almost the same as each other. The mean PWV values were 17.3, 19.4, 18.7, and 14.6 mm for spring, summer, autumn, and winter, respectively.

Figure (6) indicates the seasonal variations of the PWV during the study period and the corresponding MK results are presented in Table (4). Generally speaking, in all the seasons the PWV presented, to some extent, a decreasing trend during the considered period. However, this

Table 3
Summary of Mann-Kendall test results, Sen's slope, and the changes in the PWV values at the seven sites considered for the twelve months. Changes (%) of the PWV value for the specific time compared to the 32-year mean PWV of the corresponding time are given in the last column.

Month	Test Z	Significance	Sen's Slope Q	[Millimetres per selected period in years]	Changes [%] of PWV trend compared to the average of the considered month
January	−0.795		−0.04	−1.28	−8.26
February	0.1		0.001	0.03	0.02
March	−1.8	+	−0.08	−2.60	−16.81
April	−1.151		−0.04	−1.40	−7.80
May	−1.67	+	−0.05	−1.73	−8.80
June	−0.341		−0.01	−0.47	−2.92
July	0.4054		0.02	0.52	2.66
August	0.78		0.001	0.03	0.08
September	0.9858		0.03	0.88	4.55
October	−0.374		−0.02	−0.59	−3.20
November	−0.544		−0.03	−1.05	−5.70
December	−0.952		−0.05	−1.54	−9.65

** Trend at $\alpha = 0.01$ level of significance; * trend at $\alpha = 0.05$ level of significance; + trend at $\alpha = 0.1$ level of significance.

trend was only significant in spring according to the MK tests. The nonappearance of clear significant trends in the remaining three seasons may be due to interannual variability and differing trends of the individual months.

During the winter season, the PWV changed by about 36%, with the maximum winter PWV value occurring in 2003 (17 mm) and the minimum (12 mm) in 2010. The PWV remains between 13 and 15 mm during the period 1986–1994, with a sharp increase of 22% during 1994–1995.

The highest spring PWV values were 20.5 mm (1985), 19.8 mm (1991), and 19.5 mm (2016), while the lowest ones were 14.5 (1999) and 14.9 mm (2002). For the rest of the period the PWV remained between 16 and 18.5 mm. The PWV varies by about 42% during spring time. During the whole period of study, the PWV during spring decreased, at the significance level of $\alpha = 0.1$, by 1.8 mm (about 10.5% of the spring mean value). The maximum summer PWV value was observed in 2003 (23.5 mm) and the minimum in 1989 (16.5 mm). The PWV varies by about 42% during this season. No obvious trend can be identified for the PWV during summer time over the whole of the study period.

The fall annual PWV values varied by about 35% and the maximum of 23 mm occurred in 2002.

3.4. PWV periodicities

In this section power spectral analyses using Fourier Transform (FT) technique were carried out to investigate the periodicities in the PWV time series. The mean monthly data of the PWV values during the period between 1985 and 2016 were used for this purpose.

Figure (7) is a Lomb periodogram for all frequencies showing the main peaks of the PWV data for all the selected sites (99% confidence levels). The spectrum presents several significant peaks with different amplitudes. The most obvious peaks are the one-year, six-month, three-month, and four-month peaks. These peaks are expected to be, in one way or another, of terrestrial origin and mainly associated with seasonal variation of the meteorological parameters such as the air temperature.

Due to the effect of high peaks which may mask the presence of other periodicities, several frequency filters were applied. Four low-frequency filters were applied to the spectrum of the PWV data. These filters were between 0.005 and 0.010 month^{-1} (Fig. 8a), between 0.007 and 0.03 month^{-1} (Fig. 8b), between 0.04 and 0.05 month^{-1} (Fig. 8c), and between 0.051 and 0.07 month^{-1} (Fig. 8d).

For the first filter, the 10.8–11-year peak clearly appears, whereas the 6.1- and 3.6-year peaks are clearly seen in the second graph. The 1.7 years and 1.3 years peaks are indicated in the last two panels (c and d) respectively. These periodicities are similar to those reported by several investigators and found in solar, interplanetary, and cosmic ray parameters (e.g., Rieger et al., 1984; Bazilevskaya et al., 2000; Mavromichalaki and Petropoulos, 1997; Kudela et al., 2002). The spectral results suggest that the obtained PWV periodicities in Arabian Peninsula are, possibly, related to the solar activities, as well as, the effect of terrestrial meteorological phenomena.

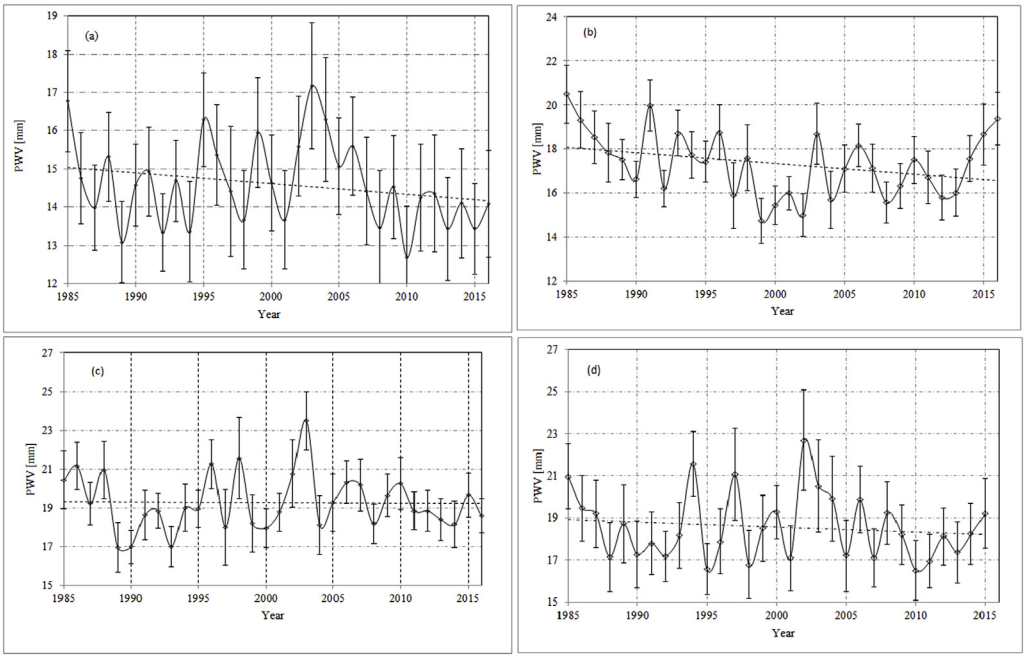

Fig. 6. Time series of the seasonal mean values of PWV (a) winter; (b) spring; (c) summer; and (d) fall in the period 1985–2016. The dashed line is the trend line.

Table 4
Summary of Mann-Kendall test results, Sen Slope, and changes in the PWV values from the seven considered sites for the four seasons. Changes (%) of the PWV value for the specific time compared to the 32-year mean PWV of the corresponding time are given in the last column.

	Test Z	Significance	Sen's slope Q	[Millimetres per selected period in years]	Changes [%] of PWV trend compared to the average of the considered season
Winter	−1.44		−0.03	−0.86	−6.11
Spring	−1.69	+	−0.06	−1.79	−10.53
Summer	−0.18		−0.01	−0.17	−0.91
Fall	−0.41		−0.01	−0.42	−2.36

+ Trend at α = 0.1 level of significance.

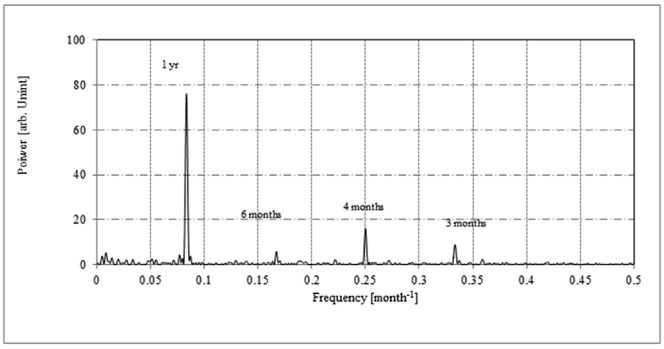

Fig. 7. Power spectrum density of the time series of the yearly mean PWV data for 1985–2016.

The heliospheric disturbances caused by the various types of solar activity affect the propagation of the high-energy cosmic rays, and in consequence, their rate at the top of the atmosphere is modulated. This modulation in the flux of the primary cosmic rays affects the level of atmospheric ionization, which results in changes in the rate of cloud formation and precipitation, according to the suggestions of several investigators (Antalovà et al., 2000; Cane et al., 1998; Kristjánsson et al., 2004; Kristjánsson et al., 2002; Marsh and Svensmark, 2000; Moraal, 1976; Pap et al., 1990; Svensmark and Friis-Christensen, 1997; Valdes-Galicia et al., 1999; Wolff, 1992). The 11-year solar cycle and its associated magnetic and cosmic ray cycles have been reported by earlier investigators (Axford, 1965; Bazilevskaya et al., 2000; Haigh 1996, 1999; Zeng, 1989; Zhao et al., 2004). Additionally, the cosmic ray periodicities of 1.3 years and 1.7 years have been recently studied and established by several researches (Joshi, 1999; Mursula and Zieger, 2000; Rieger et al., 1984; El-Borie and Al-Thoyaibd, 2002; Kudela et al., 1991; Kudela et al., 2002; Mavromichalaki and Petropoulos, 1997). The relationship between the PWV quasi periodicities and the solar activity and its impact on the cosmic rays, which affect the physical and chemical properties of the atmosphere, revealed that there are other extraterrestrial causes that may have an influence on climate change (e.g. Svensmark and Friis-Christensen, 1997; Carslaw et al., 2002). The results presented in this study are preliminary and it is recommended that more detailed investigations be carried out.

4. Conclusions

Radiosonde observations for the period 1985 to 2016 from seven sites in Saudi Arabia were used to calculate the total atmospheric water content (PWV) and to investigate its interannual, monthly, and seasonal variations. Non-parametric Mann-Kendal tests were used to detect the magnitude and trends of the PWV. A significant decrease of about 7% in the annual mean PWV is found for the entire period. A seasonal variation with a maximum during summer and minimum during winter was found in the PWV data. This type of variation may be related to the temperature variations. The PWV decreased significantly by about 1.79 mm/32 years in spring season. PWV values during March and May showed clear and significant decreasing trends with magnitudes of 2.6 mm/32 years and 1.7 mm/32 years respectively. Power spectra analyses using the Fourier Transform (FT) technique were carried out for the period 1985–2016 and revealed several long, mid, and short-term periodicities.

Short-term periodicities such as one year, six months, three months, and four months were recognized. Additionally, long and mid term periodicities such as 10.8–11 years, 1.7 years, and 1.3 years were detected. The short-term periodicities are mainly of terrestrial origin (seasonal variations). The long and mid term periodicities are similar to those reported by several investigators and found in solar, interplanetary, and cosmic ray parameters. Therefore, we suggest that the solar signals may directly or indirectly affect the long-term variations of

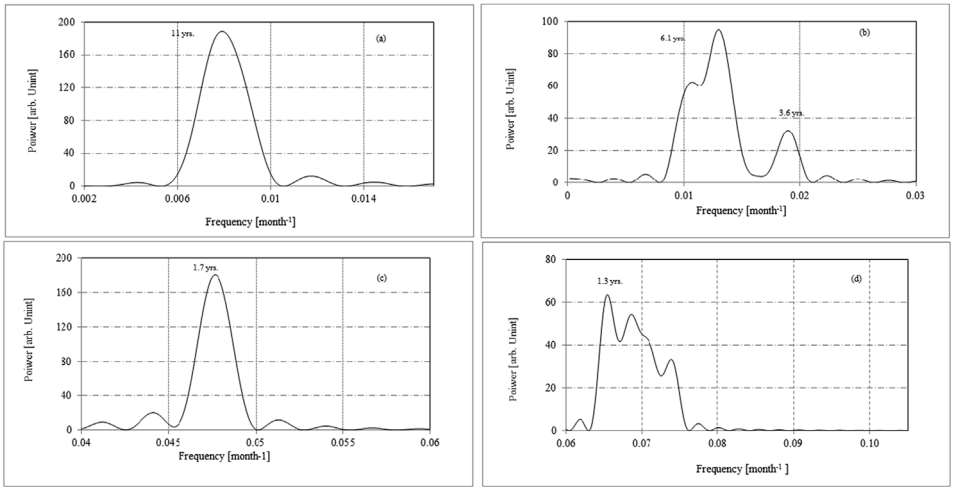

Fig. 8. The same as Figure (7) but here, low frequency filters at (a) 0.005–0.010 month^{-1}, (b) 0.007–0.03 month^{-1}, (c) 0.04–0.05 month^{-1}, and (d) 0.051–0.07 month^{-1} have been applied.

the PWV.

Acknowledgments

The authors would like to thank King Abdulaziz City for Science and Technology for supporting this work. We would also like to thank the anonymous reviewers for their comments and recommendations.

Appendix A. Supplementary data

Supplementary data to this article can be found online at https://doi.org/10.1016/j.jastp.2019.01.011.

References

Antalovà, A., Kudela, K., Rybak, J., 2000. The solar and cosmic-ray synodic periodicity (1969–1998), 2000 ESA SP-463. Space Sci. Rev. 97, 355–358.
Axford, W.I., 1965. The modulation of galactic cosmic-rays in the inter- planetary medium. Planet. Space Sci. 13, 115–130.
Bazilevskaya, G.A., Krainev, M.B., Makhmutov, V.S., Flückiger, E.O., Sladkova, A.I., Storini, M., 2000. Distribution of solar energetic particle events over an 11-year solar cycle. Sol. Phys. 197, 157–174.
Bevis, M., Businger, S., Herring, T.A., Rocken, C., Anthes, R.A., Ware, R.H., 1992. GPS meteorology, Remote sensing of atmospheric water vapour using the global positioning system. J. Geophys. Res. 97, 15784–15801.
Cane, H.V., Richardson, I.G., von Rosenvinge, T.T., 1998. Interplanetary magnetic field periodicity of ~153 days. J. Geophys. Res. 25, 4437.
Carslaw, K.S., Harrison, R.G., Kirkby, J., 2002. Cosmic rays, clouds and climate. Science 298, 1732–1737.
El-Borie, M.A., Al-Thoyaibd, S.S., 2002. Power spectrum of cosmic-ray fluctuations during consecutive. Sol. Phys. 209, 397–407.
Forster, P.M.D., Shine, K.P., 2002. Assessing the climate impact of trends in stratospheric water vapor. Geophys. Res. Lett. 29, 1086. https://doi.org/10.1029/2001GL013909.
Guerova, G., Brockmann, E., Schubiger, F., Morland, J., Mätzler, C., 2005. An integrated assessment of measured and modeled integrated water vapor in Switzerland for the period 2001– 03. J. Appl. Meteorol. 44 (7), 1033–1044.
Gueymard, C., 1994. Analysis of monthly average atmospheric precipitable water and turbidity in Canada and northern United-States. Sol. Energy 53, 57–71.
Gutzler, D., 1992. Climatic variability of temperature and humidity over the tropical western Pacific. Geophys. Res. Lett. 19, 1839–1879.
Haigh, J.D., 1996. The impact of solar variability on climate. Science 272, 981–984.
Haigh, J.D., 1999. A GCM study of climate change in response to the 11-year solar cycle. Q. J. Roy. Meteorol. Soc. 125, 871–892.
Joshi, A., 1999. Cosmic-ray periodicity at 170 days. Sol. Phys. 185, 397–403.
Kane, R.P., 1996. Interannual variability of precipitable water. Ann. Geophys. Atmos. Hydrosph. Space Sci. 14, 464–467.
Kassomenos, P.A., MCGregor, G.R., 2006. The interannual variability and trend of precipitable water over southern Greece. J. Hydrometeorol. 7, 1–14.
Kendall, M.G., 1975. Rank correlation methods, 4th ed. Charles Griffin.
Kristjánsson, J.E., Kristiansen, J., Kaas, E., 2004. Solar activity, cosmic rays, clouds and climate – an update. Adv. Space Res. 34, 407–415.
Kristjánsson, J.E., Staple, A., Kristiansen, J., Kaas, E., 2002. A new look at possible connections between solar activity, clouds and climate. Geophys. Res. Lett. 29. https://doi.org/10.1029/2002GL015646.
Kudela, K., Ananth, A.G., Venkatesan, D., 1991. The low-frequency spectral behavior of cosmic-ray intensity. J. Geophys. Res. 96, 15871–15875.
Kudela, K., Rybak, J., Antalovà, A., Storini, M., 2002. Time evolution of low-frequency periodicities in cosmic ray intensity. Sol. Phys. 205, 165–175.
Long, M., Entekhabi, D., Nicholson, S.E., 2000. Interannual variability in rainfall, water vapor flux, and vertical motion over West Africa. J. Clim. 13, 3827–3841.
Maghrabi, A.H., Clay, R.W., 2010. Precipitable water vapour estimation on the basis of sky temperatures measured by a single-pixel IR detector and screen temperatures under clear skies. 2010. J. Meteorol. Appl. 17, 279–286.
Maghrabi, A.H., Alotaib, R.N., 2017. Long-term variations of AOD from an AERONET station in the Central Arabian Peninsula. Theor. Appl. Climatol. https://doi.org/10.1007/s00704-017-2328.
Mann, H.B., 1945. Non-parametric test against trend. Econometrica 13, 245–259.
Marsh, N., Svensmark, H., 2000. Cosmic rays, clouds and climate. Space Sci. Rev. 94, 215–230.
Mavromichalaki, H., Petropoulos, B., 1997. Periodic variations or the cosmic-ray diffusion coefficient related to interplanetary and solar phenomena. In: Proc. 25th ICRC 7. pp. 313–316.
Moraal, H., 1976. Observation of the eleven-year cosmic-ray modulation cycle. Space Sci. Rev. 19, 845–920.
Mursula, K., Zieger, B., 2000. The 1.3-year variation in solar wind speed and geomagnetic activity. Adv. Space Res. 25 (9), 1939–1942.
Pap, J., Bouwer, S.D., Tobiska, W.K., Bouwer, S.D., 1990. Periodicities of solar irradiance and solar activity indices. Sol. Phys. 129, 165–189.
Pramualsakdikul, S., Haas, R., Elgered, G., Scherneck, H.G., 2007. Sensing of diurnal and semi-diurnal variability in the water vapour content in the tropics using GPS measurements. Meteorol. Appl. 14, 403–412.
Rieger, E., Share, G.H., Forrest, D.J., Kanbach, G., Reppin, C., Chupp, E.L., 1984. A 154-day periodicity in the occurrence of hard solar flares. Nature 312, 623–625.
Ruckstuhl, C., Philipona, R., Morland, J., Ohmura, A., 2007. Observed relationship between surface specific humidity, integrated water vapor, and longwave downward radiation at different altitudes. J. Geophys. Res. 112, D03302.
Singh, R.P., Mishra, N.C., Verma, A., Ramaprasad, J., 2000. Total precipitable water over the Arabian ocean and the Bay of Bengal using SSM/I data. Int. J. Rem. Sens. 21, 2497–2503.
Smirnov, V.V., Moore, G.W.K., 2001. Short-term and seasonal variability of the atmospheric water vapor transport through the Mackenzie River basin. J. Hydrometeorol. 2, 441–452.
Svensmark, H., Friis-Christensen, E., 1997. Variation of cosmic ray flux and global cloud coverage: a missing link in solar climate relationships. J. Atmos. Sol. Terr. Phys. 59, 1225–1232.
Torres, B., Cachorro, V.E., Toledano, C., Ortiz de Galisteo, J.P., Berjón, A., de Frutos, A.M., Bennouna, Y., Laulainen, N., 2010. Precipitable water vapor characterization in the Gulf of Cadiz region (southwestern Spain) based on Sun photometer, GPS, and radiosonde data. J. Geophys. Res. 115, D18103. https://doi.org/10.1029/2009JD012724. 11 PP., 2010.
Valdes-Galicia, J.F., Caballero, R., Hurtado, A., 1999. Solar cycle cosmic-ray intensity variations in the Mexico City neutron monitor. In: Proc. 26th Int. Cosmic Ray Conf., Utah, vol. 7. pp. 119–122.
Wang, J., Cole, H.L., Miller, E.R., Beierle, K., Paukkunen, A., Laine, T.K., 2002. Correction of humidity measurement errors from Vaisala RS80 radiosonde Application to TOGA COARE data. J. Atmos. Ocean. Technol. 19, 981–1002.
Wolff, C.L., 1992. Intermittent solar periodicities. Sol. Phys. 142, 187–195.
Zeng, Z.Q., 1989. Solar-Terrestrial Relationship. Seismological Press, Beijing, pp. 197.
Zhai, P., Eskridge, R.E., 1996. Analyses of inhomogeneities in radiosonde temperature and humidity time series. J. Clim. 9, 884–894.
Zhai, P., Eskridge, R.E., 1997. Atmospheric water vapor over China. J. Clim. 10, 2643–2652.
Zhao, J., Han, Yan-Ben, Li, Zhi-An, 2004. The effect of solar activity on the annual precipitation in the Beijing area Chin. J. Astron. Astrophys. 4 (2), 189–197.